

An Asymptotic Approach for Thermoelastic Analysis of Laminated Composite Plates

Wenbin Yu* and Dewey H. Hodges†

Georgia Institute of Technology, Atlanta, Georgia 30332-0150

A thermoelastic model for analyzing laminated composite plates under both mechanical and thermal loadings is constructed by the variational asymptotic method. The original three-dimensional nonlinear thermoelasticity problem is formulated based on a set of intrinsic variables defined on the reference plane and for arbitrary deformation of the normal line. Then the variational asymptotic method is used to rigorously split the three-dimensional problem into two problems: a nonlinear, two-dimensional, plate analysis over the reference plane to obtain the global deformation and a linear analysis through the thickness to provide the two-dimensional generalized constitutive law and the recovering relations to approximate the original three-dimensional results. The nonuniqueness of asymptotic theory correct up to a certain order is used to cast the obtained asymptotically correct second-order free energy into a Reissner-Mindlin type model to account for transverse shear deformation. The present theory is implemented into the computer program, Variational Asymptotic Plate and Shell Analysis (VAPAS). Results from VAPAS for several cases have been compared with the exact thermoelasticity solutions, classical lamination theory and first-order shear-deformation theory to demonstrate the accuracy and power of the proposed theory.

Keywords: Asymptotic series, anisotropic plates, finite element method, strain distribution, stress distribution, thermoelasticity

Introduction

Composite materials have found increasing applications in engineering practices due to their superior engineering properties and improving manufacturing technology. However, the heterogeneity and anisotropy of such materials make the traditional analysis method used for designing homogeneous and isotropic structures obsolete. Moreover, structures made

*Post Doctoral Fellow, School of Aerospace Engineering. Presently, Assistant Professor, Department of Mechanical and Aerospace Engineering, Utah State University, Logan Utah 84322-4130.

†Professor, School of Aerospace Engineering.

with composite materials are more sensitive and vulnerable to temperature change than their isotropic counterpart. The reason is that the thermal expansion coefficients of different constituents of the material are usually dramatically different from each other resulting in high stresses due to sudden temperature change. The analysis including thermal effects is much more involved than that for isothermal conditions.

Many engineering structures made with composite materials have one dimension much smaller than the other two and can be modeled as plates. Only a few exact solutions exist for very idealized cases (see Savoia and Reddy (1995) and the references cited there). Researchers are trying to develop simplified models to provide an approximate representation for more general cases. Within the last few decades, a tremendous research effort has been invested in this area, and various approximate models have been proposed (Wu and Tauchert (1980); Noor and Burton (1992); Reddy (1997); Noor and Malik (2000); Rohwer *et al.* (2001)). Generally speaking, these models are derived from three-dimensional (3-D) thermoelasticity theory, making use of the fact that the plate is thin in some sense. Although it is plausible to consider the smallness of the thickness of plate structures, construction of an accurate two-dimensional (2-D) model for a 3-D body still introduces a lot of challenges. Almost all the proposed models in the literature can give a good prediction of the global behavior of the plate. However, they have serious difficulties in providing accurate distributions of the 3-D displacements, strains, and stresses through the thickness. Part of the reason is that most models adopt *ad hoc* assumptions (such as having displacement or stress components vary through the thickness according to a certain function) which violate the exact solutions. For example, most high order theories (except for some layerwise theories such as Cho and Averill (2000)) assume a C^∞ continuity for the 3-D displacement field through the thickness which in reality they are piecewise continuous. In the case of thermal loading, the prediction of these *ad hoc* models become even worse, if not wrong, and the results should be examined more cautiously.

It must be understood that all plate theories, no matter how involved they may appear, are inherently approximate. The approximation lies in the 2-D constitutive law relating 2-D strains and stress resultants, which is a direct consequence of eliminating the thickness coordinate from the independent variables of the governing equations of the boundary-value problem for a plate. This sort of approximation is inevitable if one wants to take advantage of the smallness of the thickness to simplify the analysis. It is interesting to note that the 3-D constitutive relations are essentially approximate and determined by experiments. However, this cannot be used as an excuse to introduce unnecessary assumptions. For example, for small-strain analysis of plates, it is reasonable to assume that the thickness, h , is small compared to the wavelength of deformation of the reference surface, l . However, it is not at

all reasonable to assume a priori some *ad hoc* displacement field, although that is the way most plate theories are constructed.

In this paper, we first cast the original 3-D thermoelasticity problem in an intrinsic form so that the theory is applicable for arbitrarily large displacement and global rotation, subject only to the strain's being small; see Hodges *et al.* (1993). Then, the Variational Asymptotic Method (VAM), introduced by Berdichevsky (1979), is used to split the original nonlinear 3-D elasticity problem into a linear, one-dimensional (1-D), through-the-thickness analysis and a nonlinear, 2-D, plate analysis. The through-the-thickness analysis produces the 2-D constitutive law and non-mechanical stress resultants to be used in the 2-D plate analysis, along with recovering relations that yield the 3-D displacement, strain and stress fields through the thickness using results obtained from the solution of the 2-D problem. The present work extends a simple yet accurate model developed recently for composite plates and shells, namely Variational Asymptotic Plate and Shell Analysis (VAPAS) by Yu *et al.* (2002a,b, 2003) so that thermoelastic effects can be treated in the same framework.

Since the procedure is quite similar, the authors have chosen to repeat some formulae and text from their previous publications in order to make the present paper more self-contained. The present theory has been implemented into the computer program VAPAS. The hygro effects due to moisture can be treated in a similar manner as thermal effects. Thus, for simplicity of presentation, the hygro effect is not included in the formulation. It has, however, also been implemented in VAPAS. Now, one can use VAPAS along some 2-D plate solver (say, some finite element program such as DYMORE, Bauchau (1998)) to carry out an accurate and efficient hygrothermoelastic analysis for composite plates.

3-D Formulation

A point in the plate can be described by its Cartesian coordinates x_i (see Fig. 1), where x_α are two orthogonal lines in the reference plane and x_3 is the normal coordinate. (Here and throughout the paper, Greek indices assume values 1 and 2 while Latin indices assume 1, 2, and 3. Repeated indices are summed over their range except where explicitly indicated.) Letting \mathbf{b}_i denote the unit vector along x_i for the undeformed plate, one can then describe the position of any material point in the undeformed configuration by its position vector $\hat{\mathbf{r}}$ from a fixed point O , such that

$$\hat{\mathbf{r}}(x_1, x_2, x_3) = \mathbf{r}(x_1, x_2) + x_3 \mathbf{b}_3 \quad (1)$$

where \mathbf{r} is the position vector from O to the point located by x_α on the reference surface. When the reference surface of the undeformed plate coincides with its middle surface, it

naturally follows that

$$\langle \hat{\mathbf{r}}(x_1, x_2, x_3) \rangle = \mathbf{r}(x_1, x_2) \quad (2)$$

where the angle-brackets denote the definite integral through the thickness of the plate and will be used throughout the paper.

When the plate deforms, the particle that had position vector $\hat{\mathbf{r}}$ in the undeformed state now has position vector $\hat{\mathbf{R}}$ in the deformed plate. The latter can be uniquely determined by the deformation of the 3-D body. Similarly, another triad \mathbf{B}_i is introduced for the deformed configuration. The relation between \mathbf{B}_i and \mathbf{b}_i can be specified by an arbitrarily large rotation specified in terms of the matrix of direction cosines $C(x_1, x_2)$ so that

$$\mathbf{B}_i = C_{ij} \mathbf{b}_j \quad C_{ij} = \mathbf{B}_i \cdot \mathbf{b}_j \quad (3)$$

subject to the requirement that \mathbf{B}_i is coincident with \mathbf{b}_i when the structure is undeformed. Now the position vector $\hat{\mathbf{R}}$ can be represented as

$$\hat{\mathbf{R}}(x_1, x_2, x_3) = \mathbf{R}(x_1, x_2) + x_3 \mathbf{B}_3(x_1, x_2) + w_i(x_1, x_2, x_3) \mathbf{B}_i(x_1, x_2) \quad (4)$$

where w_i is the warping of the normal-line element. In the present work, the form of the warping w_i is not assumed, as in most plate theories. Rather, these quantities are treated as unknown 3-D functions and will be solved for later. Eq. (4) is six times redundant because of the way warping introduced. Six constraints are needed to make the formulation unique. The redundancy can be removed by choosing appropriate definitions of \mathbf{R} and \mathbf{B}_i . One can define \mathbf{R} similarly as Eq. (2) to be the average position through the thickness, from which it follows that the warping functions must satisfy the three constraints

$$\langle w_i(x_1, x_2, x_3) \rangle = 0 \quad (5)$$

Another two constraints can be specified by taking \mathbf{B}_3 as the normal to the reference surface of the deformed plate. It should be noted that this choice has nothing to do with the famous Kirchhoff hypothesis. Indeed, it is only for convenience in the derivation. In the Kirchhoff assumption, no local deformation of the transverse normal is allowed. On the other hand, according to the present scheme we allow all possible deformation, classifying all deformation other than that of classical lamination theory (CLT) as warping, which is assumed to be small. This assumption is valid if the strain is small and if the order of the local rotation (*i.e.* the rotation of the normal line due to warping) is of the order of the strain or smaller; see Danielson (1991).

Based on the concept of decomposition of rotation tensor, Danielson and Hodges (1987)

and Danielson (1991), the Jauman-Biot-Cauchy strain components for small local rotation are given by

$$\Gamma_{ij} = \frac{1}{2}(F_{ij} + F_{ji}) - \delta_{ij} \quad (6)$$

where F_{ij} is the mixed-basis component of the deformation gradient tensor such that

$$F_{ij} = \mathbf{B}_i \cdot \mathbf{G}_k \mathbf{g}^k \cdot \mathbf{b}_j \quad (7)$$

Here $\mathbf{G}_k = \frac{\partial \hat{\mathbf{R}}}{\partial x_k}$ is the covariant basis vector of the deformed configuration and \mathbf{g}^k the contravariant base vector of the undeformed configuration and $\mathbf{g}^k = \mathbf{g}_k = \mathbf{b}_k$. One can obtain \mathbf{G}_k with the help of the definition of so-called generalized 2-D strains similarly as Hodges *et al.* (1993), given by

$$\begin{aligned} \mathbf{R}_{,\alpha} &= \mathbf{B}_\alpha + \varepsilon_{\alpha\beta} \mathbf{B}_\beta \\ \mathbf{B}_{i,\alpha} &= (-K_{\alpha\beta} \mathbf{B}_\beta \times \mathbf{B}_3 + K_{\alpha 3} \mathbf{B}_3) \times \mathbf{B}_i \end{aligned} \quad (8)$$

where $\varepsilon_{\alpha\beta}$ and $K_{\alpha\beta}$ are the 2-D generalized strains and $(\cdot)_{,\alpha} = \frac{\partial(\cdot)}{\partial x_\alpha}$. Here one is free to set $\varepsilon_{12} = \varepsilon_{21}$, *i.e.*

$$\mathbf{B}_1 \cdot \mathbf{R}_{,2} = \mathbf{B}_2 \cdot \mathbf{R}_{,1} \quad (9)$$

which can serve as another constraint to specify the deformed configuration.

With the assumption that the strain is small compared to unity, which has the effect of removing all the terms that are products of the warping and the generalized strains, one can express the 3-D strain field as

$$\Gamma = \Gamma_h w + \Gamma_\epsilon \epsilon + \Gamma_{l_1} w_{,1} + \Gamma_{l_2} w_{,2} \quad (10)$$

where

$$\Gamma = [\Gamma_{11} \quad 2\Gamma_{12} \quad \Gamma_{22} \quad 2\Gamma_{13} \quad 2\Gamma_{23} \quad \Gamma_{33}]^T \quad (11)$$

$$w = [w_1 \quad w_2 \quad w_3]^T \quad (12)$$

$$\epsilon = [\varepsilon_{11} \quad 2\varepsilon_{12} \quad \varepsilon_{22} \quad K_{11} \quad K_{12} + K_{21} \quad K_{22}]^T \quad (13)$$

and all the operators are defined as:

$$\begin{aligned}
\Gamma_h &= \begin{bmatrix} 0 & 0 & 0 \\ 0 & 0 & 0 \\ 0 & 0 & 0 \\ \frac{\partial}{\partial x_3} & 0 & 0 \\ 0 & \frac{\partial}{\partial x_3} & 0 \\ 0 & 0 & \frac{\partial}{\partial x_3} \end{bmatrix} & \Gamma_{l_1} &= \begin{bmatrix} 1 & 0 & 0 \\ 0 & 1 & 0 \\ 0 & 0 & 0 \\ 0 & 0 & 1 \\ 0 & 0 & 0 \\ 0 & 0 & 0 \end{bmatrix} \\
\Gamma_\epsilon &= \begin{bmatrix} 1 & 0 & 0 & x_3 & 0 & 0 \\ 0 & 1 & 0 & 0 & x_3 & 0 \\ 0 & 0 & 1 & 0 & 0 & x_3 \\ 0 & 0 & 0 & 0 & 0 & 0 \\ 0 & 0 & 0 & 0 & 0 & 0 \\ 0 & 0 & 0 & 0 & 0 & 0 \end{bmatrix} & \Gamma_{l_2} &= \begin{bmatrix} 0 & 0 & 0 \\ 1 & 0 & 0 \\ 0 & 1 & 0 \\ 0 & 0 & 0 \\ 0 & 0 & 1 \\ 0 & 0 & 0 \end{bmatrix} \tag{14}
\end{aligned}$$

In the present work, we only consider one-way thermomechanical coupling and temperature change due to the deformation of the plate is negligible. Then we can use the Helmholtz free-energy functional (Reddy (1997)) without quadratic terms involving temperature only to carry out the analysis. The free energy per unit area (which is the same as the free energy of the normal-line element) can be written as

$$U = \left\langle \frac{1}{2} \Gamma^T D \Gamma - \Gamma^T D \alpha T \right\rangle \tag{15}$$

where T is the difference of temperature inside the structure with respect to the reference temperature when the plate is stress free, and D is the 3-D 6×6 material matrix, which consists of elements of the elasticity tensor expressed in the global coordinate system x_i . α is a 6×1 column matrix representing the 3-D thermal expansion coefficients. These matrices are in general fully populated. However, if it is desired to model laminated composite plates in which each lamina exhibits a monoclinic symmetry about its own mid-plane and is rotated about the local normal to be a layer in the composite laminated plate, then as shown in Yu *et al.* (2002a), some parts of these matrices will always vanish no matter what the layup angle is.

To deal with applied mechanical loads as well with thermal loads, we will at first leave open the existence of a potential energy and develop instead the virtual work of the applied mechanical loads. The virtual displacement is taken as the Lagrangean variation of the

displacement field, such that

$$\delta \hat{\mathbf{R}} = \overline{\delta q}_{Bi} \mathbf{B}_i + x_3 \overline{\delta \psi}_{Bi} \mathbf{B}_i \times \mathbf{B}_3 + \delta w_i \mathbf{B}_i + \overline{\delta \psi}_{Bi} \mathbf{B}_i \times w_j \mathbf{B}_j \quad (16)$$

where the virtual displacement of the reference surface is given by

$$\overline{\delta q}_{Bi} = \delta \mathbf{u} \cdot \mathbf{B}_i \quad (17)$$

and the virtual rotation of the reference surface is defined such that

$$\delta \mathbf{B}_i = \overline{\delta \psi}_{Bj} \mathbf{B}_j \times \mathbf{B}_i \quad (18)$$

Since the strain is small, one may safely ignore products of the warping and the loading in the virtual rotation term. Then, the work done through a virtual displacement due to the applied loads $\tau_i \mathbf{B}_i$ at the top surface and $\beta_i \mathbf{B}_i$ at the bottom surface and body force $\phi_i \mathbf{B}_i$ through the thickness is

$$\overline{\delta W} = (\tau_i + \beta_i + \langle \phi_i \rangle) \overline{\delta q}_{Bi} + \overline{\delta \psi}_{B\alpha} \left[\frac{h}{2} (\tau_\alpha - \beta_\alpha) + \langle x_3 \phi_\alpha \rangle \right] + \delta (\tau_i w_i^+ + \beta_i w_i^- + \langle \phi_i w_i \rangle) \quad (19)$$

where τ_i , β_i , and ϕ_i are taken to be independent of the deformation, $(\)^+ = (\)|_{x_3=\frac{h}{2}}$, and $(\)^- = (\)|_{x_3=-\frac{h}{2}}$. By introducing column matrices $\overline{\delta q}$, $\overline{\delta \psi}$, τ , β , and ϕ , which are formed by stacking the three elements associated with indexed symbols of the same names, and using Eqs. (1), (3), and (4), one may write the virtual work in matrix form, so that

$$\overline{\delta W} = \overline{\delta q}^T f + \overline{\delta \psi}^T m + \delta (\tau^T w^+ + \beta^T w^- + \langle \phi^T w \rangle) \quad (20)$$

where

$$f = \tau + \beta + \langle \phi \rangle$$

$$m = \left\{ \begin{array}{c} \frac{h}{2} (\tau_1 - \beta_1) + \langle x_3 \phi_1 \rangle \\ \frac{h}{2} (\tau_2 - \beta_2) + \langle x_3 \phi_2 \rangle \\ 0 \end{array} \right\} \quad (21)$$

The complete statement of the problem can now be presented in terms of the principle of virtual work, such that

$$\delta U - \overline{\delta W} = 0 \quad (22)$$

In spite of the possibility of accounting for nonconservative forces in the above, the problem that governs the warping is conservative. Thus, one can pose the problem that governs the

warping as the minimization of a total potential functional

$$\Pi = U + W \quad (23)$$

so that

$$\delta\Pi = 0 \quad (24)$$

in which only the warping displacement is varied, subject to the constraints Eq. (5). This implies that the potential of the applied mechanical loads for the functional governing warping is given by

$$W = -\tau^T w^+ - \beta^T w^- - \langle \phi^T w \rangle \quad (25)$$

Below, for simplicity of terminology, we will refer to Π as the total potential energy, or the total energy.

By principle of minimum total potential energy, one can solve for the unknown warping functions by minimizing the functional in Eq. (23) subject to the constraints of Eq. (5). Up to this point, this is simply an alternative formulation of the original 3-D elasticity problem. If we attempt to solve this problem directly, we will meet the same difficulty as solving any full 3-D elasticity problem. Fortunately, as shown in Yu *et al.* (2002a,b, 2003), the VAM can be used to calculate the 3-D warping functions asymptotically. The through-the-thickness analysis is one dimensional and can be solved analytically. However, finite element discretization is preferred to solve the minimization problem for the sake of dealing with multiple layers and arbitrary monoclinic material. A 5-noded isoparametric element is used because we need the second-order warping functions, which are piecewise, fourth-degree polynomials. Discretizing the transverse normal line into 1-D finite elements, one can express the warping field as

$$w(x_i) = S(x_3)V(x_1, x_2) \quad (26)$$

where S is the shape function and V is the nodal value of warping field along the transverse normal. Substituting Eq. (26) into Eq. (23), one can express the total energy in discretized form as

$$\begin{aligned} 2\Pi = & V^T E V + 2V^T (D_{h\epsilon}\epsilon + D_{hl_1}V_{,1} + D_{hl_2}V_{,2}) \\ & + \epsilon^T D_{\epsilon\epsilon}\epsilon + V_{,1}^T D_{l_1l_1}V_{,1} + V_{,2}^T D_{l_2l_2}V_{,2} \\ & + 2(V_{,1}^T D_{l_1\epsilon}\epsilon + V_{,2}^T D_{l_2\epsilon}\epsilon + V_{,1}^T D_{l_1l_2}V_{,2}) \\ & - 2V^T \alpha_h - 2\epsilon^T \alpha_\epsilon - 2V_{,1}^T \alpha_{l_1} - 2V_{,2}^T \alpha_{l_2} + 2V^T L \end{aligned} \quad (27)$$

where L contains the load related terms such that

$$L = -S^{+T}\tau - S^{-T}\beta - \langle S^T \phi \rangle \quad (28)$$

The new matrix variables carry the properties of both the geometry and material:

$$\begin{aligned} E &= \langle [\Gamma_h S]^T D [\Gamma_h S] \rangle & D_{h\epsilon} &= \langle [\Gamma_h S]^T D \Gamma_\epsilon \rangle \\ D_{hl_1} &= \langle [\Gamma_h S]^T D [\Gamma_{l_1} S] \rangle & D_{hl_2} &= \langle [\Gamma_h S]^T D [\Gamma_{l_2} S] \rangle \\ D_{\epsilon\epsilon} &= \langle \Gamma_\epsilon^T D \Gamma_\epsilon \rangle & D_{l_1 l_1} &= \langle [\Gamma_{l_1} S]^T D [\Gamma_{l_1} S] \rangle \\ D_{l_1 l_2} &= \langle [\Gamma_{l_1} S]^T D [\Gamma_{l_2} S] \rangle & D_{l_2 l_2} &= \langle [\Gamma_{l_2} S]^T D [\Gamma_{l_2} S] \rangle \\ D_{l_1 \epsilon} &= \langle [\Gamma_{l_1} S]^T D \Gamma_\epsilon \rangle & D_{l_2 \epsilon} &= \langle [\Gamma_{l_2} S]^T D \Gamma_\epsilon \rangle \\ \alpha_h &= \langle [\Gamma_h S]^T D \alpha T \rangle & \alpha_\epsilon &= \langle \Gamma_\epsilon^T D \alpha T \rangle \\ \alpha_{l_1} &= \langle [\Gamma_{l_1} S]^T D \alpha T \rangle & \alpha_{l_2} &= \langle [\Gamma_{l_2} S]^T D \alpha T \rangle \end{aligned} \quad (29)$$

Although the theory itself allows for an analytical representation for arbitrary temperature distribution through the thickness, here a fourth-degree polynomial is used to approximate the temperature distribution for each normal-line element. The discretized form of Eq. (5) is

$$V^T H \psi = 0 \quad (30)$$

where $H = \langle S^T S \rangle$ and ψ is the normalized kernel matrix of E such that $\psi^T H \psi = I$. Now our problem is transformed to minimize Eq. (27) numerically, subject to the constraints in Eq. (30).

Dimensional Reduction

To rigorously reduce the original 3-D problem to a 2-D plate problem, one must attempt to reproduce the energy stored in the 3-D structure in a 2-D formulation. This dimensional reduction can only be done approximately, and one way to do it is by taking advantage of the smallness of h/l . The small parameter ε , representing the order of the generalized 2-D strains ϵ has already been taken advantage of when we derive Eq. (10). To reduce the number of small parameters in the asymptotic analysis, it is reasonable to assume that the order of strains due to thermal loading is of the order ε . Thus, the quantities of interest assume the following orders:

$$\epsilon_{\alpha\beta} \sim h\kappa_{\alpha\beta} \sim \varepsilon \quad \alpha T \sim \varepsilon \quad f_3 \sim \mu(h/l)^2 \varepsilon \quad f_\alpha \sim \mu(h/l) \varepsilon \quad m_\alpha \sim \mu h(h/l) \varepsilon \quad (31)$$

where μ is the order of the material constants (all of which are assumed to be of the same order). It is noted that $m_3 = 0$.

Having assessed the orders of all the interested quantities, the VAM can be used to mathematically perform a dimensional reduction of the 3-D problem to a series of 2-D models, similarly as what have been done in Yu *et al.* (2002a,b, 2003).

The VAM requires one to find the leading terms of the functional according to the different orders. Since only the warping is varied, the leading terms needed are all of those terms associated with warping. For the zeroth-order approximation, these leading terms of Eq. (27) are

$$2\Pi_0^* = V^T EV + 2V^T D_{h\epsilon}\epsilon - 2V^T \alpha_h \quad (32)$$

The Euler-Lagrange equation for functional Eq. (32) subject to constraints Eq. (30) can be obtained by usual procedure of calculus of variation with the aid of a Lagrange multiplier as follows:

$$EV + D_{h\epsilon}\epsilon - \alpha_h = H\psi\Lambda \quad (33)$$

Considering the properties of the kernel matrix ψ , one calculates the Lagrange multiplier Λ as

$$\Lambda = \psi^T (D_{h\epsilon}\epsilon - \alpha_h) \quad (34)$$

Substituting Eq. (34) back into Eq. (33), we obtain

$$EV = (H\psi\psi^T - I)(D_{h\epsilon}\epsilon - \alpha_h) \quad (35)$$

There is a unique solution of zeroth-order warping functions and can be written as:

$$V = \hat{V}_0\epsilon + V_T = V_0 \quad (36)$$

Substituting Eq. (36) back into Eq. (27), one can obtain the total energy asymptotically correct up to the order of $\mu\epsilon^2$ as

$$2\Pi_0 = \epsilon^T (\hat{V}_0^T D_{h\epsilon} + D_{\epsilon\epsilon})\epsilon + \epsilon^T (D_{h\epsilon}^T V_T - \hat{V}_0^T \alpha_h - 2\alpha_\epsilon) \quad (37)$$

Note the quadratic terms associated with temperature $-V_T^T \alpha_h$ is dropped due to the same reason for Eq. (15). This 2-D free energy, Eq. (37), is the same as what is used in CLT for thermoelastic analysis:

$$2\Pi_0 = \epsilon^T A\epsilon - 2\epsilon^T N_T \quad (38)$$

with

$$A = (\hat{V}_0^T D_{h\epsilon} + D_{\epsilon\epsilon}) \quad N_T = \alpha_\epsilon + \frac{1}{2}(\hat{V}_0^T \alpha_h - D_{h\epsilon}^T V_T) \quad (39)$$

Although the energy of this approximation coincides with CLT, we have not used any *ad hoc* kinematic assumptions such as the Kirchhoff assumption to obtain this result. Moreover, the transverse normal strain from our zeroth-order approximation is not zero.

It is understood that our zeroth-order approximation will give the same stress results as what is obtained from CLT, *i.e.*, all the transverse stress components which are very important for analyzing the failure of composite plates cannot be predicted. One must carry out the next approximation so that those quantities can be approximately predicted. To obtain the first-order approximation, we simply perturb the zeroth-order result, resulting in warping functions of the form

$$V = V_0 + V_1 \quad (40)$$

Substituting Eq. (40) back into Eq. (10) and then into Eq. (27), one can obtain the leading terms for the first-order approximation as

$$2\Pi_1^* = V_1^T E V_1 + 2V_1^T D_1 \epsilon_{,1} + 2V_2^T D_2 \epsilon_{,2} + 2V^T L_T + 2V_1^T L \quad (41)$$

with

$$\begin{aligned} D_1 &= (D_{hl_1} - D_{hl_1}^T) \hat{V}_0 - D_{l_1\epsilon} \\ D_2 &= (D_{hl_2} - D_{hl_2}^T) \hat{V}_0 - D_{l_2\epsilon} \\ L_T &= (D_{hl_1} - D_{hl_1}^T) V_{T,1} + (D_{hl_2} - D_{hl_2}^T) V_{T,2} + \alpha_{l_1,1} + \alpha_{l_2,2} \end{aligned} \quad (42)$$

Integration by parts with respect to the in-plane coordinates is used here and hereafter whenever it is convenient for the derivation, because the present goal is to obtain an interior solution for the plate without consideration of boundary layer effects.

Similarly as in the zeroth-order approximation, one can solve the first-order warping field as

$$V_1 = V_{11}\epsilon_{,1} + V_{12}\epsilon_{,2} + V_{1T} + V_{1L} \quad (43)$$

and obtain a total energy that is asymptotically correct up to the order of $\mu(h/l)^2\epsilon$, given by

$$2\Pi_1 = \epsilon^T A \epsilon + \epsilon_{,1}^T B \epsilon_{,1} + 2\epsilon_{,1}^T C \epsilon_{,2} + \epsilon_{,2}^T \mathcal{D} \epsilon_{,2} + 2\epsilon^T F - 2\epsilon^T F_T \quad (44)$$

where

$$\begin{aligned}
B &= \hat{V}_0^T D_{l_1 l_1} \hat{V}_0 + V_{11}^T D_1 & C &= \hat{V}_0^T D_{l_1 l_2} \hat{V}_0 + \frac{1}{2}(V_{11}^T D_2 + D_1^T V_{11}) \\
\mathcal{D} &= \hat{V}_0^T D_{l_2 l_2} \hat{V}_0 + V_{12}^T D_2 & F &= \hat{V}_0^T L - \frac{1}{2}(D_1^T V_{1L,1} + V_{11}^T L_{,1} + D_2^T V_{1L,2} + V_{12}^T L_{,2})
\end{aligned} \tag{45}$$

with the non-mechanical load due to temperature

$$\begin{aligned}
F_T &= N_T + \hat{V}_0^T D_{l_1 l_1} V_{T,11} + \hat{V}_0^T D_{l_2 l_2} V_{T,22} + \hat{V}_0^T (D_{l_1 l_2} + D_{l_1 l_2}^T) V_{T,12} \\
&\quad + \frac{1}{2}(V_{11}^T L_{T,1} + V_{12}^T L_{T,2} + D_1^T V_{1T,1} + D_2^T V_{1T,2})
\end{aligned} \tag{46}$$

Here the monoclinic symmetry has already been taken advantage of to obtain the asymptotically correct energy in Eq. (44). The applied mechanical loads and temperature distribution should not vary rapidly over the plate surface; otherwise the structure, although plate-like, can not be analyzed with enough accuracy using a reduced plate model.

Transforming Into Reissner-Mindlin Model

Although Eq. (44) is asymptotically correct through the second order and straightforward use of this free energy expression is possible, it involves more complicated boundary conditions than necessary since it contains derivatives of the generalized strain measures. To obtain an energy functional that is of practical use, one can transform the present approximation into a Reissner-Mindlin type model. We would like to state that fitting the asymptotic energy into such model is just a choice, and the possibility of fitting the same energy into other more sophisticated plate models is under investigation.

In a Reissner-Mindlin model, there are two additional degrees of freedom, which are the transverse shear strains. These are incorporated into the rotation of transverse normal. If we introduce another triad \mathbf{B}_i^* for the deformed Reissner-Mindlin plate, the definition of 2-D strains becomes

$$\begin{aligned}
\mathbf{R}_{,\alpha} &= \mathbf{B}_\alpha^* + \varepsilon_{\alpha\beta}^* \mathbf{B}_\beta^* + 2\gamma_{\alpha 3} \mathbf{B}_3^* \\
\mathbf{B}_{i,\alpha}^* &= (-K_{\alpha\beta}^* \mathbf{B}_\beta^* \times \mathbf{B}_3^* + K_{\alpha 3}^* \mathbf{B}_3^*) \times \mathbf{B}_i^*
\end{aligned} \tag{47}$$

where the transverse shear strains are $\gamma = [2\gamma_{13} \quad 2\gamma_{23}]^T$. From the definitions in Eqs. (8) and (47), one can obtain the Rodrigues parameters corresponding to the rotation relating \mathbf{B}_i and \mathbf{B}_i^* . Using the procedures listed in Hodges (1987), one can express the classical strain measures ϵ in terms of the strain measures of the Reissner-Mindlin plate model (see

Yu (2002) for the details of the derivation):

$$\epsilon = \mathcal{R} - \mathcal{D}_\alpha \gamma, \alpha \quad (48)$$

where

$$\begin{aligned} \mathcal{D}_1 &= \begin{bmatrix} 0 & 0 & 0 & 1 & 0 & 0 \\ 0 & 0 & 0 & 0 & 1 & 0 \end{bmatrix}^T \\ \mathcal{D}_2 &= \begin{bmatrix} 0 & 0 & 0 & 0 & 1 & 0 \\ 0 & 0 & 0 & 0 & 0 & 1 \end{bmatrix}^T \\ \mathcal{R} &= [\varepsilon_{11}^* \quad 2\varepsilon_{12}^* \quad \varepsilon_{22}^* \quad K_{11}^* \quad K_{12}^* + K_{21}^* \quad K_{22}^*]^T \end{aligned} \quad (49)$$

Now one can express the energy, Eq. (44), correct to second order, in terms of strains of the Reissner-Mindlin model as

$$\begin{aligned} 2\Pi_1 &= \mathcal{R}^T A \mathcal{R} - 2\mathcal{R}^T A \mathcal{D}_\alpha \gamma, \alpha + \mathcal{R}_{,1}^T B \mathcal{R}_{,1} + 2\mathcal{R}_{,1}^T C \mathcal{R}_{,2} + \mathcal{R}_{,2}^T D \mathcal{R}_{,2} \\ &+ 2\mathcal{R}^T F - 2R^T F_T + 2\gamma_\alpha^T D_\alpha N_T \end{aligned} \quad (50)$$

The generalized Reissner-Mindlin model used in the 2-D thermoelastic analyses is of the form

$$2\Pi_{\mathcal{R}} = \mathcal{R}^T A \mathcal{R} + \gamma^T G \gamma + 2\mathcal{R}^T F_{\mathcal{R}} + 2\gamma^T F_\gamma + 2\mathcal{R}^T F_{T\mathcal{R}} + 2\gamma^T F_{T\gamma} \quad (51)$$

To find an equivalent Reissner model Eq. (51) for Eq. (50), one has to eliminate all partial derivatives of the classical 2-D strain measures. The equilibrium equations are used to achieve this purpose. From the two equilibrium equations balancing bending moments with applied moments m_α which is calculated from Eq. (21), one can obtain the following formula

$$G\gamma + F_\gamma + F_{T\gamma} = \mathcal{D}_\alpha^T (A\mathcal{R}_{,\alpha} + F_{\mathcal{R},\alpha} + F_{T\mathcal{R},\alpha}) + \begin{Bmatrix} m_1 \\ m_2 \end{Bmatrix} \quad (52)$$

Using Eq. (52), one can rewrite Eq. (50) as

$$2\Pi_1 = \mathcal{R}^T A \mathcal{R} + \gamma^T G \gamma + 2\mathcal{R}^T F - 2\mathcal{R}^T F_T - 2\gamma^T \mathcal{D}_\alpha N_{T,\alpha} + U^* \quad (53)$$

where

$$U^* = \mathcal{R}_{,1}^T \bar{B} \mathcal{R}_{,1} + 2\mathcal{R}_{,1}^T \bar{C} \mathcal{R}_{,2} + \mathcal{R}_{,2}^T \bar{D} \mathcal{R}_{,2} \quad (54)$$

and

$$\begin{aligned}
\bar{B} &= B + A\mathcal{D}_1G^{-1}\mathcal{D}_1^T A \\
\bar{C} &= C + A\mathcal{D}_1G^{-1}\mathcal{D}_2^T A \\
\bar{D} &= D + A\mathcal{D}_2G^{-1}\mathcal{D}_2^T A
\end{aligned} \tag{55}$$

If we can drive U^* to zero for any \mathcal{R} , then we have found an asymptotically correct Reissner-Mindlin plate model. For generally anisotropic plates, this term will not be zero; but we can minimize the error to obtain a Reissner-Mindlin model that is as close to asymptotical correctness as possible. The accuracy of the Reissner-Mindlin model depends on how close to zero one can drive this term of the energy.

One could proceed with the optimization at this point, but the problem will require a least squares solution for 3 unknowns (the shear stiffness matrix G) from a linear system of 78 equations (12×12 and symmetric). This optimization problem is too rigid. The solution will be better if we can bring more unknowns into the problem. As stated in Sutyrin and Hodges (1996), there is no unique plate theory of a given order. One can relax the constraints in Eq. (5) to be $\langle w_i \rangle = \text{const}$ and still obtain an asymptotically correct strain energy. Since the zeroth-order approximation gives us an asymptotic model corresponding to classical plate theory, we only relax the constraints for the first-order approximation. This relaxation will modify the warping field to be

$$\bar{V}_1 = V_{11}\epsilon_{,1} + V_{12}\epsilon_{,2} + V_{1L} + V_{1T} + L_1\epsilon_{,1} + L_2\epsilon_{,2} \tag{56}$$

where L_1, L_2 consist of 24 constants. The remaining energy U^* will also be modified to be

$$U^* = \mathcal{R}_{,1}^T \hat{B} \mathcal{R}_{,1} + 2\mathcal{R}_{,1}^T \hat{C} \mathcal{R}_{,2} + \mathcal{R}_{,2}^T \hat{D} \mathcal{R}_{,2} \tag{57}$$

and

$$\hat{B} = \bar{B} + 2L_1^T D_1 \quad \hat{C} = \bar{C} + (L_1^T D_2 + D_1^T L_2) \quad \hat{D} = \bar{D} + 2L_2^T D_2 \tag{58}$$

Since now we have 27 unknowns, the optimization is much more flexible. It can give us a more optimal solution for the shear stiffness matrix G to fit the second-order, asymptotically correct energy into a Reissner-Mindlin model. In other words, here we have found the Reissner-Mindlin model that describes as closely as possible the 2-D energy that is asymptotically correct through the second order in h/l . However, the asymptotical correctness of the warping field to that same order can only be ascertained after obtaining another higher-order approximation, which will be discussed in the next section.

And after minimizing U^* , the “best” total energy to be used for the 2-D plate Reissner-Mindlin model can be expressed as:

$$2\Pi_{\mathcal{R}} = \mathcal{R}^T A \mathcal{R} + \gamma^T G \gamma + 2\mathcal{R}^T F - 2\mathcal{R}^T F_T - 2\gamma^T \mathcal{D}_\alpha N_{T,\alpha} \quad (59)$$

Recovering Relations

From the above, we have obtained a Reissner-Mindlin plate model which is as close as possible to being asymptotically correct in the sense of matching the total energy. The stiffness matrices A , G , load-related terms, and non-mechanical stress resultants can be used as input for a plate theory derived from the total energy obtained here. The geometrically nonlinear theory presented in Hodges *et al.* (1993) is an appropriate choice, but some straightforward modification of the loading terms is required.

However, while it is necessary to accurately calculate the 2-D displacement field of composite plates, this is not sufficient in many applications. Ultimately, *the fidelity of a reduced-order model such as this depends on how well it can predict the 3-D results in the original 3-D problem.* Hence, recovering relations should be provided to complete the reduced-order model. By recovering relations, we mean expressions for 3-D displacement, strain, and stress fields in terms of 2-D quantities and x_3 . For validation, results obtained for the 3-D field variables from the reduced-order model must be compared with those of the original 3-D model.

For an energy that is asymptotically correct through the second order, we can recover the 3-D displacement, strain and stress fields only through the first order in the strict sense of asymptotical correctness. Using Eqs. (1), (3), and (4), one can recover the 3-D displacement field through the first order as

$$U_{3d} = u_{2d} + x_3 \begin{bmatrix} C_{31} \\ C_{32} \\ C_{33} - 1 \end{bmatrix} + S V_0 + S \bar{V}_1 \quad (60)$$

where U_{3d} is the column matrix of 3-D displacements and u_{2d} is the plate displacements. C_{ij} are the components of global rotation tensor from Eq. (3). And from Eq. (10), one can recover the 3-D strain field through the first order as

$$\Gamma = \Gamma_h S (V_0 + \bar{V}_1) + \Gamma_\epsilon \epsilon + \Gamma_{l_1} S V_{0,1} + \Gamma_{l_2} S V_{0,2} \quad (61)$$

Then, one can use the inverse of 3-D Duhamel-Neumann law

$$\sigma = D\Gamma - D\alpha T \quad (62)$$

to obtain 3-D stresses σ_{ij} .

Since we have obtained an optimum shear stiffness matrix G , some of the recovered 3-D results through the first order are better than classical theory and conventional first-order deformation theory. However, for the transverse normal component of strain and stress (*i.e.* Γ_{33} and σ_{33}), the agreement is not satisfactory at all. Let us recall, that the Reissner-Mindlin theory that has been constructed only ensures a good fit with the asymptotically correct 3-D displacement field of the first order (while energy is approximated to the second order). Thus, in order to obtain recovering relations that are valid to the same order as the energy, the VAM iteration needs to be applied one more time.

Using the same procedure listed in previous section, the second-order warping can be obtained and expressed symbolically as

$$V_2 = V_{21}\epsilon_{,11} + V_{22}\epsilon_{,12} + V_{23}\epsilon_{,22} + V_{2L} + V_{2T} \quad (63)$$

Eq. (63) is obtained by taking the original first-order warping V_1 to be the result of the first-order approximation. It is clear that V_2 is one order higher than V_1 which confirms that V_1 is the first-order approximation. One might be tempted to use V_1 in the recovering relations. However, the VAM has split the original 3-D problem into two sets of problems. As far as recovering relations concerned, it is observed that the normal-line analysis can at best give us an approximate shape of the distribution of 3-D results. The 2-D plate analysis will govern the global behavior of the structure. Since \bar{V}_1 is the warping that yields a Reissner-Mindlin plate model that is as close as possible to being asymptotically correct, we should still use \bar{V}_1 in the recovering relations instead of V_1 . By doing this, we choose to be more consistent with Reissner-Mindlin plate model while compromising somewhat on the asymptotical correctness of the shape of the distribution. It has been verified by numerical examples that this is a good choice.

Hence, we write the 3-D recovering relations for displacement through the second order as

$$U_{3d} = u_{2d} + x_3 \left\{ \begin{array}{c} C_{31} \\ C_{32} \\ C_{33} - 1 \end{array} \right\} + S(V_0 + \bar{V}_1 + V_2) \quad (64)$$

and the strain field through the second order is

$$\Gamma = \Gamma_h S(V_0 + \bar{V}_1 + V_2) + \Gamma_\epsilon \epsilon + \Gamma_{l_1} S(V_{0,1} + \bar{V}_{1,1}) + \Gamma_{l_2} S(V_{0,2} + \bar{V}_{1,2}) \quad (65)$$

Again the stresses through the second order can be obtained from use of the 3-D constitutive law, Eq. (62).

Numerical Examples

The computer program VAPAS has been extended to implement the present theory. Several numerical examples are given here to validate the proposed theory and code against the 3-D thermoelasticity solutions.

First to assess the asymptotical correctness of the proposed theory, we study a cylindrical bending type problem for an isotropic plate with E as the Young's modulus, ν Poisson's ratio and α thermal expansion coefficient. The plate is simply supported with width L along x_1 axis (the "lateral" direction) and infinitely long along the x_2 axis (the "longitudinal" direction) under the following temperature changes:

$$T = T_0(x_3) \sin\left(\frac{\pi x_1}{L}\right) \quad (66)$$

Let us assume the thickness of the plate is h , and the normalized thickness coordinate $\zeta = x_3/h$, then the small parameter used in our theory is:

$$\delta = \frac{h}{l} = \frac{\pi h}{L} \quad (67)$$

When there is a uniform temperature T_c change through the thickness, the nontrivial displacements and stresses are listed in Table 1. The exact solutions are obtained based on Savoia and Reddy (1995) and expanded into a series in terms of δ with $o(*)$ denoting terms asymptotically smaller than the order of $*$. The present theory can predict the correct results up to the second order of δ with respect to the leading terms for each 3-D quantities, which clearly demonstrate that our theory is asymptotically correct up to the second order for this particular problem. We admit that the prediction of transverse components for this problem is out of the power of our theory. However, this should not mislead the reader to assume that the present theory is asymptotically correct up to the second order for general cases. The authors are aware that the proposed theory can be at best asymptotically correct up to the second order for particular cases. For general cases, however, the theory can only be interpreted as a Reissner-Mindlin type theory which is closest to being asymptotically correct. To illustrate the above statement, we provide the results for the same isotropic plate

under a linearly distributed temperature through the thickness, assuming $T_0 = \zeta T_1$. Here only nontrivial displacement results are listed in Table 2 which is sufficient for the aforementioned purpose. One can observe from Table 2 that there is a slight difference for the second order prediction between the present theory and exact solution. It is interesting to note that if one sets ν equal to zero the difference disappears. Evidently some information belonging to second order and indeed included in the asymptotically correct energy cannot be captured in a Reissner-Mindlin type model. When we transform the asymptotically correct model into a Reissner-Mindlin model, this information is lost.

The present theory is formulated with sufficient generality to carry out a thermoelastic analysis for arbitrary composite laminated plates made with monoclinic material with a computational cost equivalent to that of first-order shear-deformation theory (FOSDT). Hence, before overemphasizing the loss of information in the repackaging of the model one should determine if this loss is exhibited in numerical results. To investigate this, we will present some numerical results for composite plates to demonstrate the advantages of our theory relative to CLT and FOSDT. The plate we are going to study has material properties given by

$$\begin{aligned}
E_L &= 172.4 \text{ GPa} \quad (25 \times 10^6 \text{ psi}) & E_T &= 6.895 \text{ GPa} \quad (10^6 \text{ psi}) \\
G_{LT} &= 3.447 \text{ GPa} \quad (0.5 \times 10^6 \text{ psi}) & G_{TT} &= 1.379 \text{ GPa} \quad (0.2 \times 10^6 \text{ psi}) \\
\nu_{LT} &= 0.25 & \nu_{TT} &= 0.25 \\
\alpha_L &= 0.139 \times 10^{-6} / ^\circ C & \alpha_T &= 9 \times 10^{-6} / ^\circ C
\end{aligned} \tag{68}$$

For the purpose of comparing with the exact solution, we still consider cylindrical bending type problem. In lieu of our definition of small parameter Eq. (67), even if our theory is asymptotically correct up to the second order, we require $\delta^3 \ll 1$. If we assume the thickness is 25.4 mm and $L = 254$ mm, δ will be approximately 0.314 which can be considered small in our theory. Two different cases are investigated:

- case 1: nearly cross ply, $[-0.5^\circ/89.5^\circ]$ under $T_0 = T_c + \zeta T_c$
- case 2: nearly cross ply, $[90.5^\circ/0.5^\circ/90.5^\circ/0.5^\circ]$ under $T_0 = T_c + \zeta T_c + \zeta^2 T_c + \zeta^3 T_c + \zeta^4 T_c$
 $\tau_3 = \beta_3 = \frac{p_0}{2} \sin\left(\frac{\pi x_1}{L}\right)$, $\tau_\alpha = \beta_\alpha = 0$, and $p_0 = E_T \alpha_T T_c / 9$.

Because thermal stresses due to temperature change are the most interesting quantities, we only present stress results here with mentioning that the accuracy of displacements and strains is similar to that of stresses. For case 1, results from VAPAS (dots in the plots), are compared with those from CLT (dash-dotted line), FOSDT (dashed line) and the exact solution (solid line) in Figs. 2 – 7. Note that, because the 2-D variables are either sine

functions or cosine functions, $\sigma_{\alpha\beta}$ and σ_{33} are plotted at $x_1 = L/2$ and $\sigma_{\alpha 3}$ at $x_1 = L$. The results presented here are normalized as follows:

$$\bar{\sigma}_{ij} = \frac{9\sigma_{ij}}{E_T\alpha_T T_c} \quad (69)$$

As one can observe from the plots, for $\sigma_{\alpha\beta}$ VAPAS results are much closer to the exact solutions than CLT and FOSDT. VAPAS also does a fairly good job for predicting the transverse stress components which for the isotropic plate under uniform temperature change we concluded was out of the power of VAPAS because these terms are asymptotically smaller than the second order. One can infer that due to the special layup scheme (cross-ply) the dominant terms of transverse stress components could now be asymptotically equal or larger than the second order. Considering the smallness of σ_{33} in comparison to the in-plane components, we expect the slight shift of VAPAS results for this quantity to be tolerable for most engineering applications.

Finally, to demonstrate that VAPAS can handle the temperature change through the thickness exactly up to a fourth-degree polynomial and both mechanical loads and thermal load can be treated simultaneously, we present the results for case 2 in Figs. 8 – 13. Except for a small shift for transverse normal stress, all the other results from VAPAS are almost on top of the exact solutions. Careful readers may even find there is a small discontinuity for σ_{33} which should not be the case in reality. The reason is due to that the stress results obtained by VAPAS are calculated directly using 3-D constitutive law from the approximate strain field. The approximation in the strain field may cause the discontinuity for the transverse stress components. It is worthy to emphasize that integration of the 3-D equilibrium equations through the thickness is not used here to obtain results for the transverse stresses presented herein, in contrast to what is usually done in CLT and FOSDT.

Mathematically, the accuracy of the present theory should be comparable to that of a reduced layer-wise plate theory with assumed in-plane displacements as layer-wise cubic polynomials of the thickness direction and transverse displacement as a layer-wise fourth-degree polynomial. However, the present theory is still an equivalent single-layer theory, and the computational requirement is much less than that for layer-wise theories.

Conclusion

A Reissner-Mindlin type plate model capable of performing a thermoelastic stress analysis of laminated composite plates has been constructed by the variational-asymptotic method. A general 2-D constitutive law being as close to asymptotical correctness as possible has been obtained by solving the 1-D through-the-thickness analysis. The original 3-D results have

been reproduced as accurate as possible from a Reissner-Mindlin type plate analysis. The resulting theory is as simple and efficient as a first-order shear deformation theory (FOSDT) while it also has an accuracy comparable to higher-order layerwise theories.

The present study distinguishes from previous work reported in the literature at least in the following four aspects:

1. The present formulation is in an intrinsic form which is suitable for geometrically nonlinear plate theory as well as linear theory.
2. The dimensional reduction from 3-D to 2-D is carried out systematically by using variational asymptotic method, which is completely different from models that rely on the introduction of *ad hoc* kinematic assumptions to reduce the dimensionality.
3. To create a smooth interface with well-established 2-D solvers, the degrees of freedom of the present model are chosen to be essentially the same as those of traditional Reissner-Mindlin type plate theory. However, the present model is *not* a FOSDT. The present theory differs from FOSDT by representing all the deformations that are purposely eliminated in the development of FOSDT. This is accomplished through allowing all possible deformation in the 3-D warping functions, which are solved in turn by the variational-asymptotic method.
4. The present study has treated both mechanical and thermal loading. The temperature distribution through the thickness can be arbitrary and is approximated in VAPAS by a layerwise fourth-degree polynomial. This is more realistic and accurate than most published models, in which the temperature is assumed to be distributed linearly through the thickness of the whole plate (single-layer theories) or a layer (for layerwise theories).

The hygro effect due to moisture to composite plates can also be handled in exactly the same procedure except one has to replace the thermal expansion coefficients with hygroscopic expansion coefficients and temperature with moisture. The computer program VAPAS can now be used along with a 2-D solver to perform an efficient yet accurate and detailed analysis for hygrothermoelastic behavior for laminated composite plates under severe environments.

Acknowledgements

This research is supported by the Air Force Office of Scientific Research, USAF, under grant F49620-01-1-0038 (Maj. William M. Hilbun, technical monitor). The views and conclusions contained herein are those of the authors and should not be interpreted as necessarily representing the official policies or endorsement, either expressed or implied, of AFOSR or the U.S. Government.

References

- Bauchau, O. (1998). Computational schemes for flexible, nonlinear multi-body systems. *Multibody System Dynamics* 2, 169–225.
- Berdichevsky, V. L. (1979). Variational-asymptotic method of constructing a theory of shells. *PMM* 43, 664 – 687.
- Cho, Y. B. and Averill, R. C. (2000). First-order zig-zag sublaminated plate theory and finite element model for laminated composite and sandwich panels. *Composite Structures* 50, 1 – 15.
- Danielson, D. A. (1991). Finite rotation with small strain in beams and plates. In Proceedings of the 2nd Pan American Congress of Applied Mechanics. Valparaiso, Chile. Valparaiso Chile.
- Danielson, D. A. and Hodges, D. H. (1987). Nonlinear beam kinematics by decomposition of the rotation tensor. *Journal of Applied Mechanics* 54, 258 – 262.
- Hodges, D. H. (1987). Finite rotation and nonlinear beam kinematics. *Vertica* 11, 297 – 307.
- Hodges, D. H., Atilgan, A. R. and Danielson, D. A. (1993). A geometrically nonlinear theory of elastic plates. *Journal of Applied Mechanics* 60, 109 – 116.
- Noor, A. K. and Burton, S. W. (1992). Computational models for high-temperature multi-layered composite plates and shells. *Applied Mechanics Reviews* 45, 419–446.
- Noor, A. K. and Malik, M. (2000). An assessment of five modeling approaches for thermo-mechanical stress analysis of laminated composite panels. *Computational Mechanics* 25, 43–58.
- Reddy, J. N. (1997). *Mechanics of Laminated Composite Plates: Theory and Analysis*. CRC Press, Boca Raton, Florida.
- Rohwer, K., Rolfes, R. and Sparr, H. (2001). Higher-order theories for thermal stresses in layered plates. *International Journal of Solids and Structures* 38, 3673–3687.
- Savoia, M. and Reddy, J. N. (1995). Three-dimensional thermal analysis of laminated composite plates. *International Journal of Solids and Structures* 32, 593–608.
- Sutyrin, V. G. and Hodges, D. H. (1996). On asymptotically correct linear laminated plate theory. *International Journal of Solids and Structures* 33, 3649 – 3671.

- Wu, C. and Tauchert, T. (1980). Thermoelastic analysis of laminated plates. part I: symmetric specially orthotropic laminates. *Journal of Thermal Stresses* 3, 247–259.
- Yu, W. (2002). Variational asymptotic modeling of composite dimensionally reducible structures. Ph.D. thesis, Aerospace Engineering, Georgia Institute of Technology.
- Yu, W., Hodges, D. H. and Volovoi, V. V. (2002a). Asymptotic construction of Reissner-like models for composite plates with accurate strain recovery. *International Journal of Solids and Structures* 39, 5185 – 5203.
- Yu, W., Hodges, D. H. and Volovoi, V. V. (2002b). Asymptotic generalization of Reissner-Mindlin theory: accurate three-dimensional recovery for composite shells. *Computer Methods in Applied Mechanics and Engineering* 191, 5087 – 5109.
- Yu, W., Hodges, D. H. and Volovoi, V. V. (2003). Asymptotically accurate 3-d recovery from Reissner-like composite plate finite elements. *Computers and Structures* 81, 439 – 454.

List of Tables

1	3-D displacements and stresses under uniform temperature change through the thickness	24
2	3-D displacements under linearly distributed temperature change through the thickness	25

Table 1: 3-D displacements and stresses under uniform temperature change through the thickness

Normalized lateral displacement ($\frac{u}{hT_c\alpha}$)	
Exact	$-\frac{(\nu+1)}{\pi}\delta^{-1} - \frac{\pi(12\zeta^2-1)(\nu+1)}{24}\delta + \frac{\pi^3[120\zeta^2(1-2\zeta^2)(\nu^2-\nu-2)+\nu^2+15\nu+14]}{5760(\nu-1)}\delta^3 + o(\delta^4)$
Present	$-\frac{(\nu+1)}{\pi}\delta^{-1} - \frac{\pi(12\zeta^2-1)(\nu+1)}{24}\delta + o(\delta)$
Normalized transverse displacement ($\frac{w}{hT_c\alpha}$)	
Exact	$(\nu+1)\zeta + \frac{\pi^2\zeta(4\zeta^2-1)\nu(\nu+1)}{24(\nu-1)}\delta^2 + \frac{\pi^4\zeta[8\zeta^2(6\zeta^2-5)(\nu+1)^2-\nu^2+14\nu+15]}{5760(\nu-1)\delta^4} + o(\delta^4)$
Present	$(\nu+1)\zeta + \frac{\pi^2\zeta(4\zeta^2-1)\nu(\nu+1)}{24(\nu-1)}\delta^2 + o(\delta^2)$
Normalized lateral in-plane stress ($\frac{\sigma_{11}}{ET_c\alpha}$)	
Exact	$-\frac{\pi^2(12\zeta^2-1)}{24(\nu-1)}\delta^2 - \frac{\pi^4(240\zeta^4-120\zeta^2+7)}{2880(\nu-1)}\delta^4 + o(\delta^4)$
Present	$-\frac{\pi^2(12\zeta^2-1)}{24(\nu-1)}\delta^2 + o(\delta^2)$
Normalized longitudinal in-plane stress ($\frac{\sigma_{22}}{ET_c\alpha}$)	
Exact	$-1 - \frac{\pi^2(12\zeta^2-1)\nu}{24(\nu-1)}\delta^2 + \frac{\pi^4(-240\zeta^4+120\zeta^2+1)\nu}{5760(\nu-1)}\delta^4 + o(\delta^4)$
Present	$-1 - \frac{\pi^2(12\zeta^2-1)\nu}{24(\nu-1)}\delta^2 + o(\delta^2)$
Normalized lateral transverse shear stress ($\frac{\sigma_{13}}{ET_c\alpha}$)	
Exact	$\frac{\pi^3\zeta(4\zeta^2-1)}{24(\nu-1)}\delta^3 + o(\delta^4)$
Present	Not available
Normalized transverse normal stress ($\frac{\sigma_{33}}{ET_c\alpha}$)	
Exact	$\frac{\pi^4(4\zeta^2-1)^2}{384(\nu-1)}\delta^4 + o(\delta^4)$
Present	Not available

Table 2: 3-D displacements under linearly distributed temperature change through the thickness

Normalized lateral displacement ($\frac{u}{hT_1\alpha}$)	
Exact	$-\frac{\zeta(\nu+1)}{\pi}\delta^{-1} - \frac{\pi\zeta(20\zeta^2-3)(\nu+1)}{120}\delta + o(\delta)$
Present	$-\frac{\zeta(\nu+1)}{\pi}\delta^{-1} - \frac{\pi\zeta(20\zeta^2-3)(\nu+1)}{120}\delta + \frac{\pi\zeta\nu(11\nu^4+2\nu^3+8\nu^2+14\nu-3)}{30(11\nu^4-12\nu^3+34\nu^2-12\nu+11)}\delta + o(\delta)$
Normalized transverse displacement ($\frac{w}{hT_1\alpha}$)	
Exact	$\frac{\nu+1}{\pi^2}\delta^{-2} + \frac{1}{40}(20\zeta^2-1)(\nu+1) + o(\delta^0)$
Present	$\frac{\nu+1}{\pi^2}\delta^{-2} + \frac{1}{40}(20\zeta^2-1)(\nu+1) - \frac{\nu(11\nu^4+2\nu^3+8\nu^2+14\nu-3)}{30(11\nu^4-12\nu^3+34\nu^2-12\nu+11)} + o(\delta^0)$

List of Figures

1	Schematic of plate deformation	27
2	Distribution of the 3-D stress σ_{11} vs the thickness coordinate (case 1)	28
3	Distribution of the 3-D stress σ_{12} vs the thickness coordinate (case 1)	29
4	Distribution of the 3-D stress σ_{22} vs the thickness coordinate (case 1)	30
5	Distribution of the 3-D stress σ_{13} vs the thickness coordinate (case 1)	31
6	Distribution of the 3-D stress σ_{23} vs the thickness coordinate (case 1)	32
7	Distribution of the 3-D stress σ_{33} vs the thickness coordinate (case 1)	33
8	Distribution of the 3-D stress σ_{11} vs the thickness coordinate (case 2)	34
9	Distribution of the 3-D stress σ_{12} vs the thickness coordinate (case 2)	35
10	Distribution of the 3-D stress σ_{22} vs the thickness coordinate (case 2)	36
11	Distribution of the 3-D stress σ_{13} vs the thickness coordinate (case 2)	37
12	Distribution of the 3-D stress σ_{23} vs the thickness coordinate (case 2)	38
13	Distribution of the 3-D stress σ_{33} vs the thickness coordinate (case 2)	39

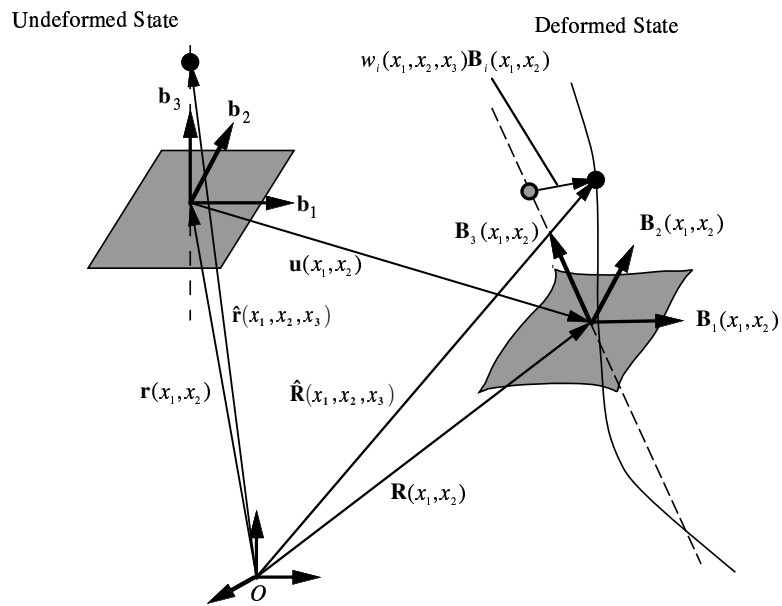


Figure 1: Schematic of plate deformation

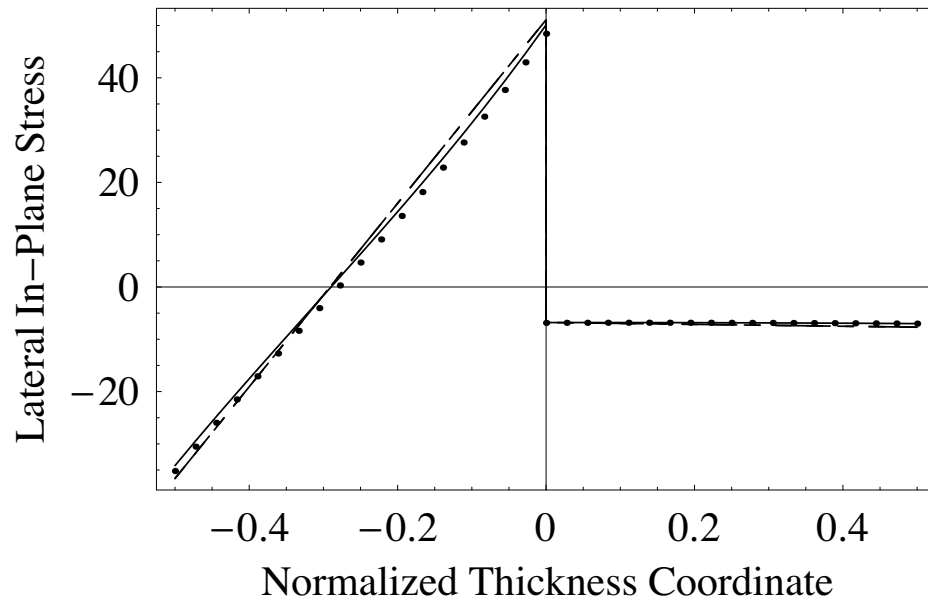


Figure 2: Distribution of the 3-D stress σ_{11} vs the thickness coordinate (case 1)

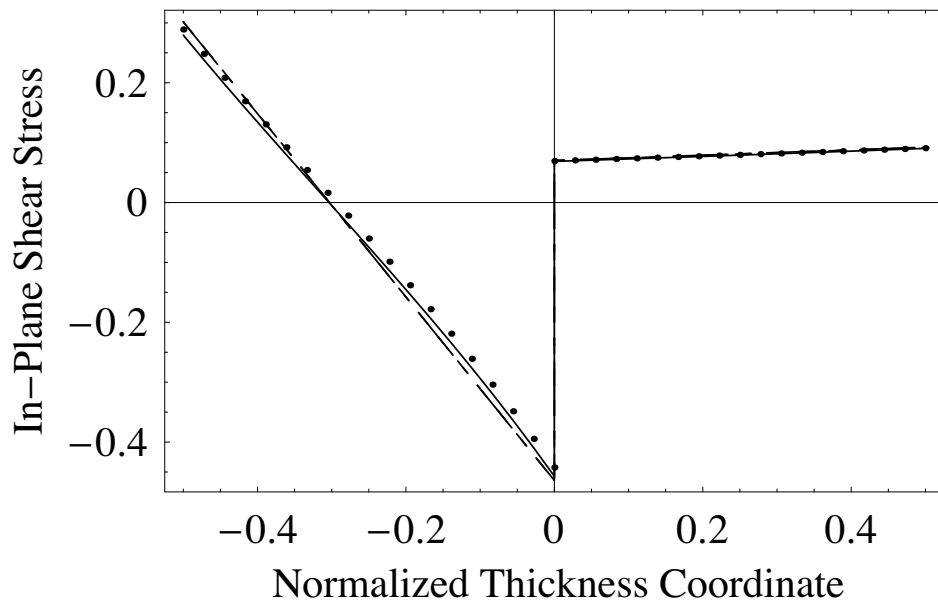


Figure 3: Distribution of the 3-D stress σ_{12} vs the thickness coordinate (case 1)

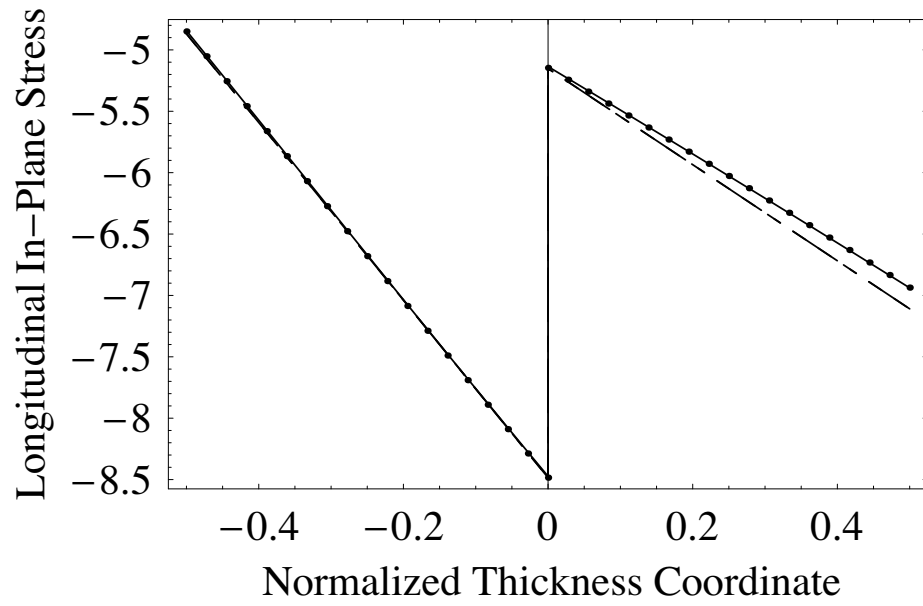


Figure 4: Distribution of the 3-D stress σ_{22} vs the thickness coordinate (case 1)

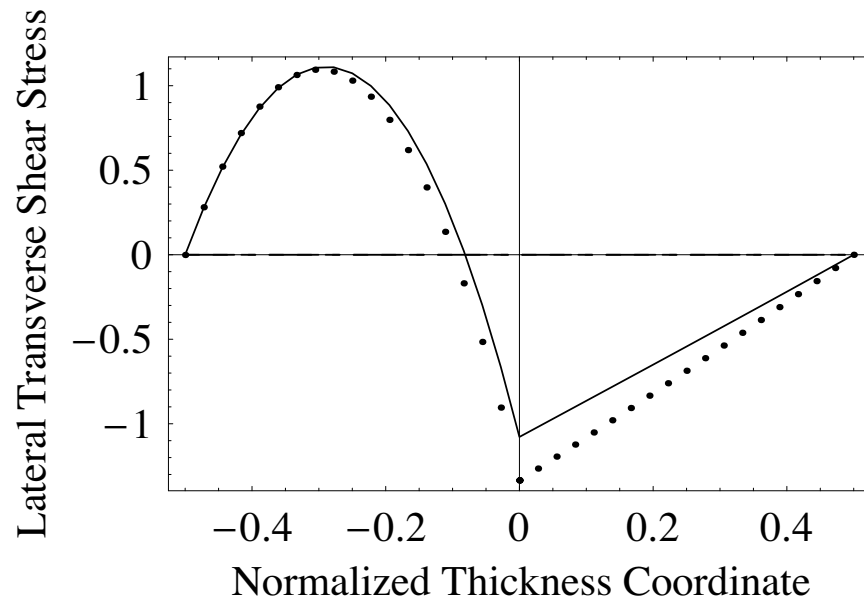


Figure 5: Distribution of the 3-D stress σ_{13} vs the thickness coordinate (case 1)

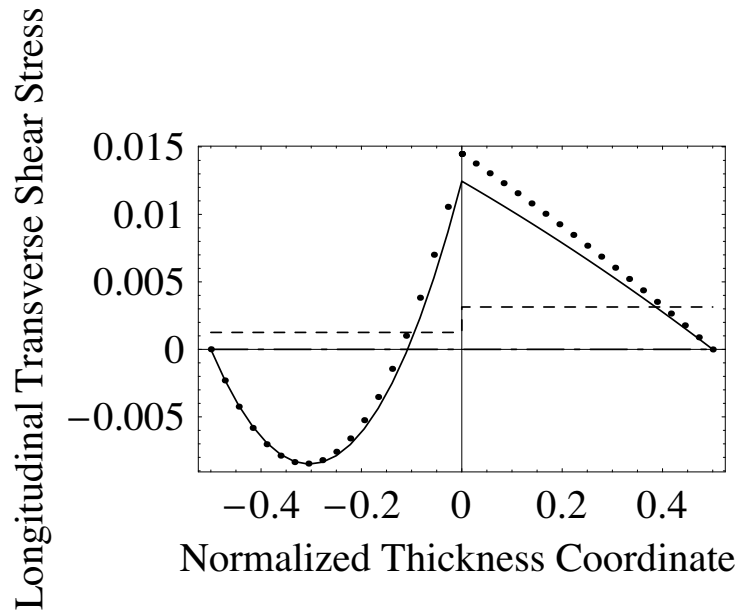


Figure 6: Distribution of the 3-D stress σ_{23} vs the thickness coordinate (case 1)

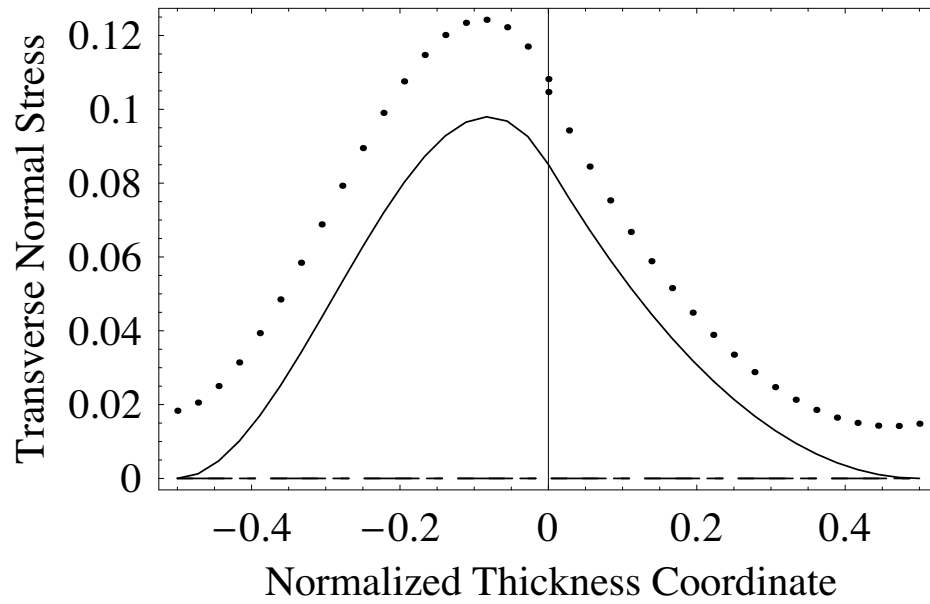


Figure 7: Distribution of the 3-D stress σ_{33} vs the thickness coordinate (case 1)

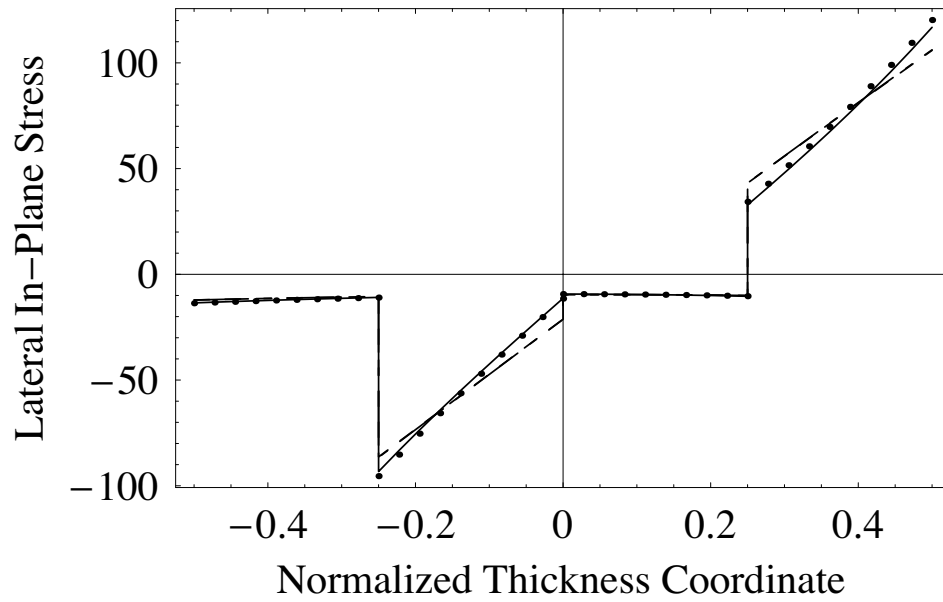


Figure 8: Distribution of the 3-D stress σ_{11} vs the thickness coordinate (case 2)

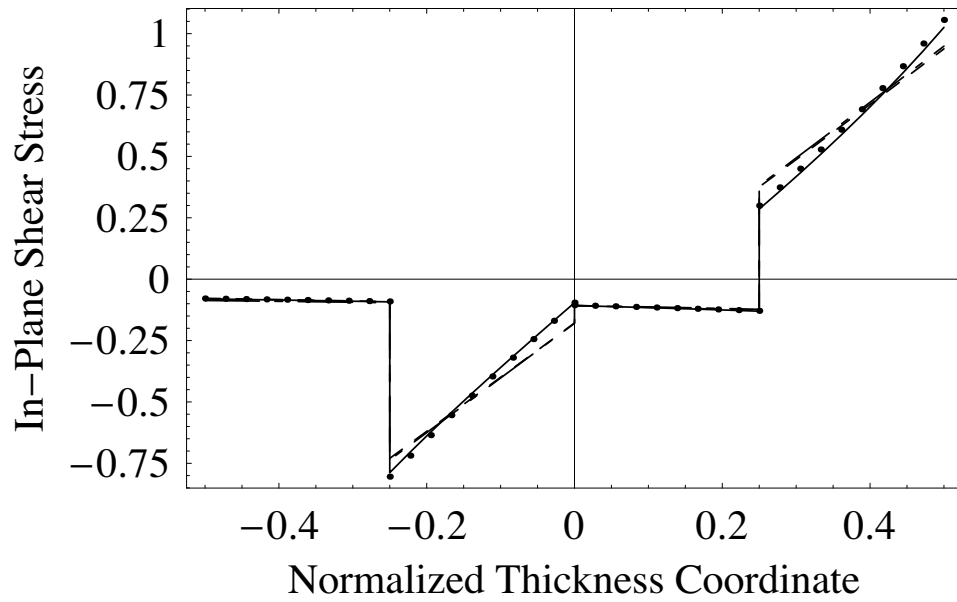


Figure 9: Distribution of the 3-D stress σ_{12} vs the thickness coordinate (case 2)

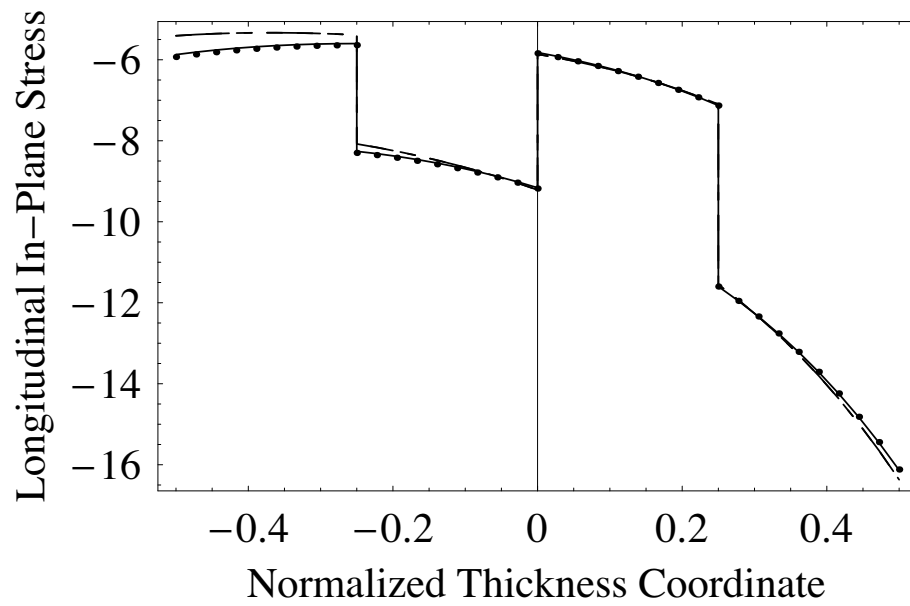


Figure 10: Distribution of the 3-D stress σ_{22} vs the thickness coordinate (case 2)

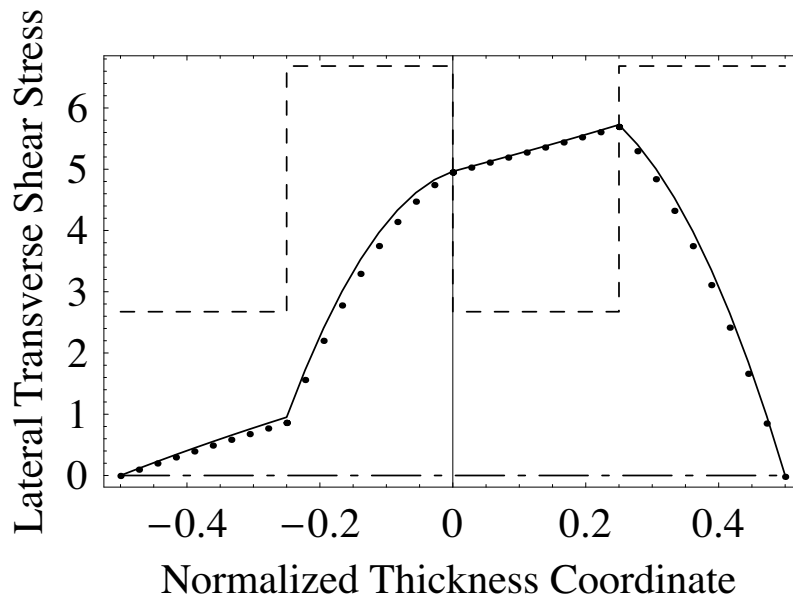


Figure 11: Distribution of the 3-D stress σ_{13} vs the thickness coordinate (case 2)

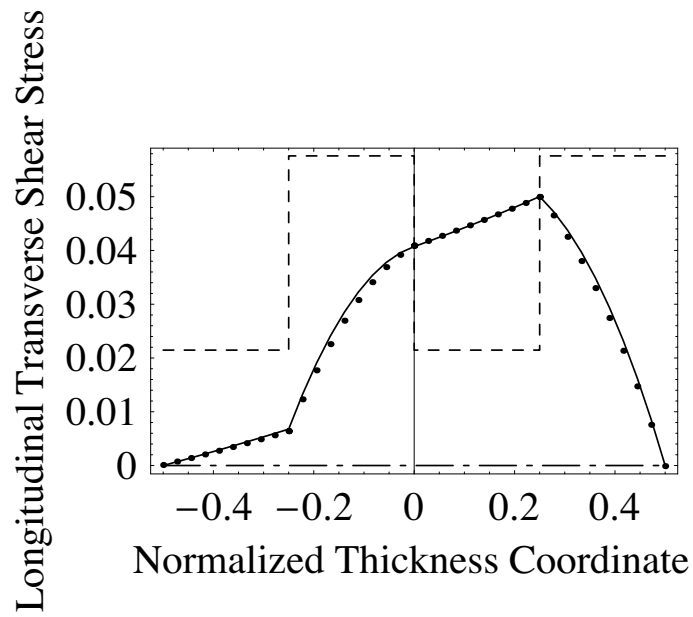


Figure 12: Distribution of the 3-D stress σ_{23} vs the thickness coordinate (case 2)

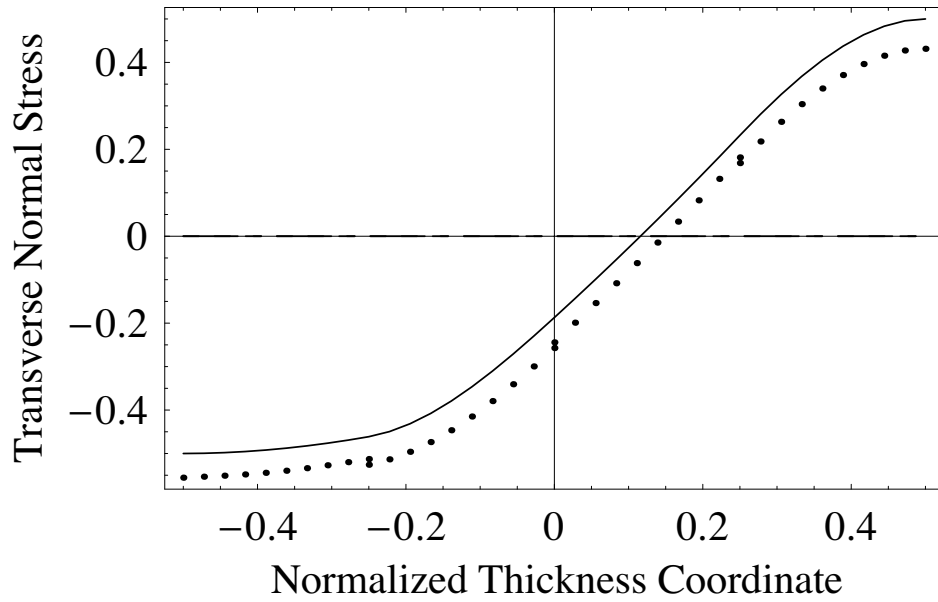


Figure 13: Distribution of the 3-D stress σ_{33} vs the thickness coordinate (case 2)